Third International Conference on CFD in the Minerals and Process Industries
CSIRO, Melbourne, Australia
10-12 December 2003

SIMULATION OF THE CAKE FORMATION AND GROWTH IN SEDIMENTATION AND FILTRATION

K. J. DONG[1], R.Y. YANG[1], R. P. ZOU[1], A. B. YU[1], G. ROACH[2] and E. JAMIESON[2]

[1] Centre for Simulation and Modelling of Particulate Systems, School of Materials Science and Engineering
The University of New South Wales, Sydney, NSW 2052, Australia

[2] Technology Delivery Group, Alcoa World Alumina, Cockburn Road, Kwinana, WA 6167, Australia

ABSTRACT

This paper presents a numerical study of the cake formation and growth in sedimentation or filtration in which the flow of discrete particles is three-dimensional and the flow of continuous liquid one-dimensional. The motion of particles is controlled by various forces, including particle-particle interactions due to collision and the van der Waals forces between particles, and particle-fluid interactions such as buoyancy, drag and lift forces. The validity of the method is tested by comparing the simulated and measured results. It is shown this simulation technique can generate detailed information at both microscopic and macroscopic levels. The cake thickness, average cake solidosity, filtrate volume, filtrate flow rate (for constant pressure filtration) or pressure drop across the filter unit (for constant rate filtration) as a function of filtrate time have been quantified under different flow and operational conditions. The effects of variables such as particle size, Hamaker constant, fluid density and fluid viscosity on cake properties are examined through a series of controlled numerical experiments.

INTRODUCTION

Sedimentation and filtration are the solid-liquid separation processes widely used in the chemical and mineral industries. Separated from the slurry (mixture of particles and liquid), particles will eventually form a packed bed known as 'cake'. Cake formation and structure are very important to the process and have been subjected to research for decades. For instance, cake resistance in filtration, which directly affects the performance of the process, is mainly determined by the structure of the cake. To fully understand the cake structure, it is required to study the cake formation and growth at a particle level. However, such microscopic information will be difficult to obtain either with the phenomenological theories (Burger, et al., 2001) or the current experimental techniques.

Several semi-dynamic methods were developed in the past to overcome this difficulty. Houi and Lenormand (1986) proposed a sticking model to describe the 2D deposition of spheres on the filter medium. Tassopoulos et al. (1989) developed a discrete stochastic model to consider the probability of particle deposition on a substrate surface. Later on, Lu and co-workers (Lu and Hwang, 1993; Lu et al. 1993; Lu and Hwang, 1995) developed a kinematic model to simulate the whole process of cake formation. In their model, force balance on a single particle was considered, including gravity force and particle-fluid forces. While these models have revealed some micro mechanisms of the cake formation, they are based on assumptions for stable state and therefore not fully dynamic models.

On the other hand, the discrete element method (DEM) is based on Newton's equations of motion, providing a first principal approach to describe the motion of individual particles in a considered system. While the DEM model was originally used in environments absent of fluid, increasingly efforts have been made to extend this model to the mixture of fluid and particles. The successful coupling of DEM with CFD (computational fluid dynamics) in the study of gas-solid flow has proved the applicability of the DEM model in the fluid environment as recently reviewed by Yu and Xu (2003). Recent experimental work of the forces between particles in liquid environment (Zhao and Davis, 2002) has also made the extension of the DEM model to the systems of the mixtures of particles and liquids possible.

In this paper, the DEM model is extended to simulate sedimentation and filtration. The cake formation and growth will be discussed. The effect of liquid and particle properties such as liquid density, liquid viscosity and Hamaker constant on cake formation and structure will also be studied.

MODEL DESCRIPTION

In DEM simulation, a particle possesses the translational and rotation motion which can be described by:

$$m_i \frac{d\mathbf{v}_i}{dt} = \mathbf{F}_i \tag{1}$$

$$I_i \frac{d\boldsymbol{\omega}_i}{dt} = \mathbf{T}_i \tag{2}$$

where $\mathbf{v}_i$, $\boldsymbol{\omega}_i$, m_i and I_i are, respectively, the transitional and angular velocities, mass and moment of inertia of particle i; $\mathbf{F}_i$ and $\mathbf{T}_i$ are the total forces and torques acting on the particle (Fig. 1). In the present work, the total force and torque are given by:

$$\mathbf{F}_i = \sum \left(\mathbf{F}_{ij}^n + \mathbf{F}_{ij}^s + \mathbf{F}_{ij}^v \right) + \mathbf{F}_{buoy} + \mathbf{F}_{drag} + \mathbf{F}_{lift} + m_i \mathbf{g} \tag{3}$$

$$\mathbf{T}_i = \sum_j \left(\mathbf{R}_i \times \mathbf{F}_{ij}^s - \mathbf{T}_{ij}^r \right) \tag{4}$$

where $\mathbf{F}^n$, $\mathbf{F}^s$, $\mathbf{F}^v$, $\mathbf{F}_{buoy}$, $\mathbf{F}_{drag}$ and $\mathbf{F}_{lift}$ are, respectively, normal contact force, tangential contact force, van der Waals force, buoyancy force, drag force and lift force.

$\mathbf{T}_{ij}^r$ ($=-\mu_r R_i \left|\mathbf{F}_{ij}^n\right| \hat{\boldsymbol{\omega}}$) is the torque caused by rolling friction due to the elastic hysteresis losses or viscous dissipation between colliding particles.

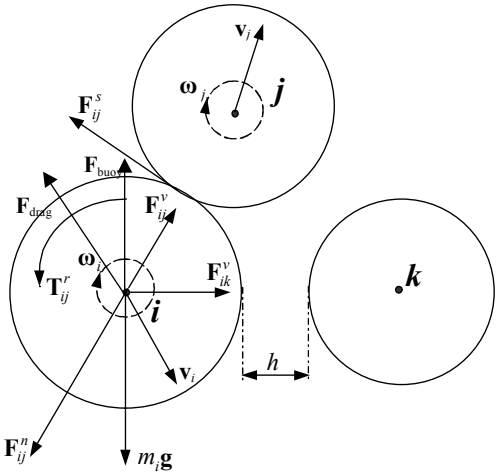

Figure 1. Schematic illustrations of the forces exerting on particle *i*

The normal and tangential contact forces can be given by (Brilliantov et al., 1996; Johnson, 1985; Langston et al., 1995):

$$\mathbf{F}_{ij}^n = \left[\frac{2}{3}E\sqrt{\overline{R}}\xi_n^{\frac{3}{2}} - \gamma_n E\sqrt{\overline{R}}\sqrt{\xi_n}\left(\mathbf{v}_{ij}\cdot\hat{\mathbf{n}}_{ij}\right)\right]\hat{\mathbf{n}}_{ij} \tag{5}$$

$$\mathbf{F}_{ij}^s = -\operatorname{sgn}\left(\xi_s\right)\mu_s\left|\mathbf{F}_{ij}^n\right|\left[1-\left(1-\frac{\min\left(\xi_s,\xi_{s,\max}\right)}{\xi_{s,\max}}\right)\right] \tag{6}$$

where $E = Y/(1-\tilde{\sigma}^2)$ and Y and $\tilde{\sigma}$ are, respectively, Young's modulus and Poisson ratio; ξ_n is the overlap between particles i and j; $\hat{\mathbf{n}}_{ij}$ is a unit vector running from the centre of particle *j* to the centre of particle *i*;. The normal damping constant, γ_n, can be treated as a material property directly linked to the normal coefficient of restitution. ξ_s and $\xi_{s,max}$ are, respectively, the total and maximum tangential displacements of particle i during contact.

The particle size considered in this work is down to micron meters; therefore the van der Waals force is also taken into account to describe the long-range cohesive force. This is given by (Israelachvili, 1991):

$$\mathbf{F}_{ij}^v = -\frac{H_a}{6}\cdot\frac{64R_i^3R_j^3(h+R_i+R_j)}{(h^2+2R_ih+2R_jh)^2(h^2+2R_ih+2R_jh+4R_iR_j)^2}\hat{\mathbf{n}}_{ij} \tag{7}$$

While it is recognised that an overlap between two colliding particles is possible in DEM, a minimum separation h_{min} is assumed in the present work. This is necessary in order to represent the physical repulsive nature between particles and avoid the singular attractive force when h equals zero (Yang et al. 2000). For simplicity the electrostatic and Brownian forces are ignored.

To extend the DEM model to the fluid-particle system, the interaction between particles and fluids should be incorporated. There is a range of forces involved (Crowe et al., 1998). However, not all are important in particular application. In this work, three forces are considered, i.e. buoyancy, drag and lift forces, given by (Xu et al., 2000; Crowe et al., 1998).

$$\mathbf{F}_{buoy} = mg\frac{\rho_f}{\rho_p} \tag{8}$$

$$\mathbf{F}_{drag,i} = \mathbf{f}_{f0,i}\varepsilon_i^{-(\chi+1)} \tag{9}$$

$$\mathbf{F}_{lift} = \frac{\pi}{8}\rho_f R_i^3(1-\varepsilon_i)[(\frac{1}{2}\nabla\times\mathbf{u}_f-\boldsymbol{\omega}_i)\times(\mathbf{u}_f-\mathbf{u}_i)] \tag{10}$$

where

$$\mathbf{f}_{f0,i} = 0.5c_{d0,i}\rho_f\pi R_i^2\varepsilon_i^2\left|\mathbf{u}_f-\mathbf{u}_i\right|(\mathbf{u}_f-\mathbf{u}_i) \tag{11}$$

$$\chi = 3.7-0.65\exp\left[-\frac{(1.5-\log_{10}\mathrm{Re}_{p,i})^2}{2}\right] \tag{12}$$

$$C_{d0,i} = (0.63+\frac{4.8}{\mathrm{Re}_{p,i}^{0.5}})^2 \tag{13}$$

$$\mathrm{Re}_{p,i} = \frac{2\rho_f R_i\varepsilon_i\left|\mathbf{u}_f-\mathbf{u}_i\right|}{\mu_f} \tag{14}$$

In this case local porosity ε_i is assumed to depend on height only. Thus, the simulated box can be sliced into pieces along the sediment direction. The particles in a slice have the same local porosity.

SIMULATION CONDITIONS

This work concerns the sedimentation and filtration processes. In the simulation, two assumptions of fluid flow were made: (i) liquid flow is one-dimensional; and (ii) the liquid flow rate is constant across the sedimentation/filtration bed. In the sedimentation process the liquid velocity is set to zero while in the filtration simulation the liquid velocity relates to the flow-rate and is a function of the cake porosity and the pressure, calculated from the well-known Carman-Kozeny equation (Svarovsky, 2000):

$$\Delta p = \frac{5\mu_f L_c(1-\varepsilon_c)^2 S_0^2}{\varepsilon_c^3}u_{slurry} \tag{15}$$

where L_c , ε_c , and S_0 are the thickness, porosity and specific surface area of the cakes respectively, u_{slurry} is the flow rate. In this model, the simulated box will be sliced into pieces along the sediment direction. Each slice has its own average porosity. So the total pressure drop due to the presence of particles should be the sum of the pressure across each sector, i.e.

$$\Delta p = \sum_i \Delta p_i = \sum_i \frac{5\mu_f L_{c,i}(1-\varepsilon_{c,i})^2 S_{0,i}^2}{\varepsilon_{c,i}^3}u_{slurry} \tag{16}$$

where the subscript *i* represents the *i*th piece.

A simulation begins with the random generation of mono-sized spherical particles with no overlap in a rectangular box with a width of 15 particle diameters. Then, the

particles will be allowed to settle down under the gravity and other forces to form a cake. Table 1 lists the physical conditions and parameters for the present simulation. Most of the parameters have been successfully used in the simulation of dry particles (Yang et al. 2000). As such, the present work focuses on the effects of liquid-related properties.

Table 1. Parameters in the simulation

Parameter	Value
Particle size, D_p	20 – 2000 μm
Particle density, ρ_p	2.46×10^3 kg/m^3
Particle number, N	2250
Young's modulus, Y	1.0×10^6 N m^2
Poisson's ratio, $\tilde{\sigma}$	0.29
Sliding friction coefficient, μ_s	0.3
Rolling friction coefficient, μ_r	0.002
Liquid Density, ρ_f	$1.0 – 2.45 \times 10^3$ kg/m^3
Liquid Viscosity, μ_f	0.0001238 – 0.1238 kg/ms
Hamaker constant, H_a	$1.0 \times 10^{-22} – 6.5 \times 10^{-20}$ J
Minimum gap, h_{min}	1 nm

RESULTS AND DISCUSSION

Model validation

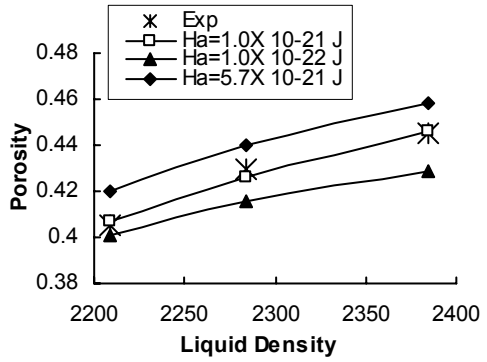

Figure 2. Comparison of simulated and experimental results for porosity under different liquid density.

To validate the proposed model, simulations were made under similar conditions to those used in the experimental study of Onoda and Liniger (1990) in which glass beads were settled in the mixture of diiodomethane and toluene. In the simulation the Hamaker constant is the only adjustable parameter. This is because the Hamaker constant has different values in different media. Although the Hamaker constant for glass beads is well known when the medium is air (6.5×10^{-20}J) or water (0.57×10^{-20}J), no empirical data is available for the liquid mixture currently used. Therefore, we varied its value in the simulation. It can be seen from Fig. 2 that when the Hamaker constant is 1.0×10^{-21}J, the simulation can accurately reproduce the experimental data. The agreement between simulation and experimental data also indicates the applicability of the numerical model. Note that although here porosity is plotted as a function of liquid density, viscosity of a liquid mixture also varies with its composition, which has been taken the present simulations.

Cake formation

To study the effect of particle and liquid properties on the cake formation in a sedimentation process, several simulations were performed with different liquid density, viscosity and Hamaker constant. Figures 3-5 show the cake thickness and porosity as a function of time under different simulation conditions during the sedimentation process. It can be seen from these figures that cake thickness increases almost linearly with time, which is qualitatively in good agreement with present theories of sedimentations (Garrido et al., 2000). It is also shown that the cake porosity has a steep decrease at the beginning and quickly reaches a stable value which is similar to that of the so called loose random packing (Yang et al., 2000).

The results also show that the increase of liquid density (Fig. 3) or viscosity (Fig. 4) increases the sedimentation time. On the other hand, the Hamaker constant (Fig. 5) has very small effect on the sedimentation time but causes larger differences in cake porosity, which will be discussed further in sections 4.2 and 4.3.

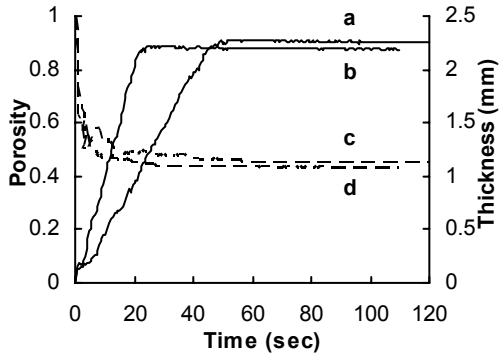

Figure 3. Cake porosity (dash line) and thickness (solid line) as a function of time for different liquid density when $D_p = 250$ μm, $H_a = 0.57 \times 10^{-20}$ J, μ_f = 0.001238kg/ms: (a) and (c) are cake thickness and porosity for ρ_f =1500kg/m^3; (b) and (d) thickness and porosity for ρ_f = 500 kg/m^3.

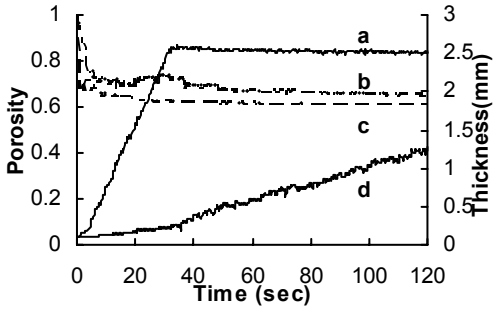

Figure 4. Cake porosity (dash line) and thickness (solid line) as a function of time for different liquid viscosity when $D_p = 250\mu m$, $H_a = 0.57 \times 10^{-20}$ J, $\rho_f = 10^3$ kg/m^3: (a) and (c) are cake thickness and porosity when $\mu_f = 1.238\times 10^{-4}$ kg/ms; (b) and (d) thickness and porosity when $\mu_f = 1.238\times 10^{-3}$ kg/ms.

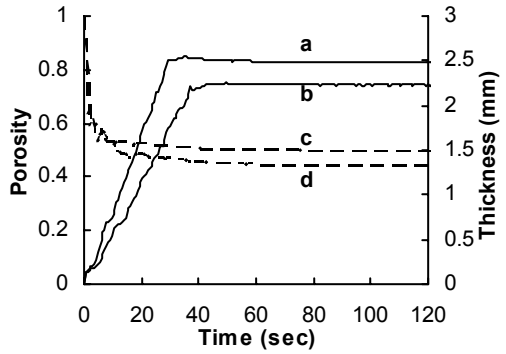

Figure 5. Cake porosity (dash line) and thickness (solid line) a function of time for different Hamaker constant when $D_p = 250\mu m$, $\mu_f = 1.238\times10^{-3}$kg/ms, $\rho_f = 1000$kg/m^3: (a) and (c) are cake thickness and porosity when $H_a = 6.5 \times 10^{-20}$ J; (b) and (d) thickness and porosity when $H_a = 0.57 \times 10^{-20}$ J.

Two types of filtration were simulated: constant flow rate and constant pressure. In the constant flow rate filtration the velocity of the slurries remains unchanged while the pressure drop increases with time. Figure 6 shows the effect of Hamaker constant on the pressure, indicating higher values of Hamaker constant will slow the increase of pressure drop. This is because cake porosity can be as high as 0.60 with $H_a = 6.5 \times 10^{-20}$ J and decrease to 0.46 when Hamaker constant equals 5.7×10^{-21} J.

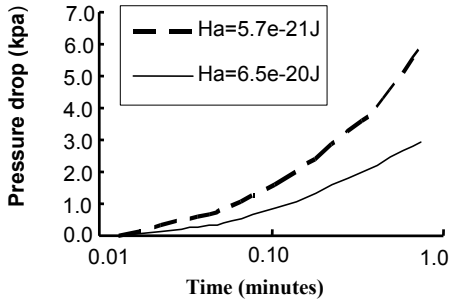

Figure 6. Pressure drop as a function of filtration time for different Hamaker constant when $D_p = 20$ μm, $\rho_f = 1.0 \times 10^3$ kg/m^3, $\mu_f = 0.001238$ kg/ms, $U_f = 0.01$ m/s.

In constant pressure filtration, two stages can be observed: At the first stage, the slurry possesses a constant flow rate similar to the initial flow rate as the cake accretes; at the second stage when the pressure drop reaches its preset maximum, the flow rate decreases to keep the pressure drop constant. Figure 7 shows the flow rate as a function of time at different pressure drops, which agrees qualitatively with the experimental results (Svarovsky, 2000). Figure 8 shows the cake thickness and porosity at two pressure drops. It can be seen that the higher the pressure drop, the faster the filtration. Yet the pressure has very little effect on the cake solidosity (porosity).

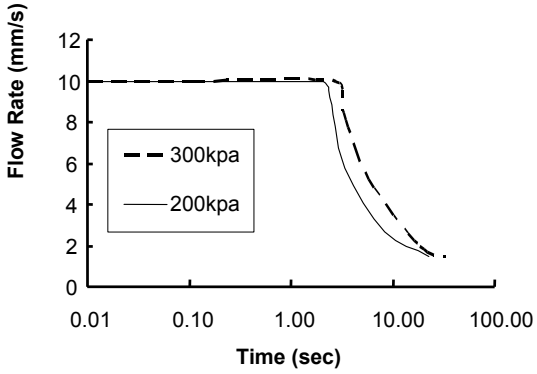

Figure 7. Flow rate as a function of filtration time for different pressure drop when $D_p = 20$ μm, $\rho_f = 1.0 \times 10^3$ kg/m^3, $\mu_f = 0.001238$ kg/ms, $H_a = 5.7 \times 10^{-21}$ J, $U_{f,0} = 0.01$m/s.

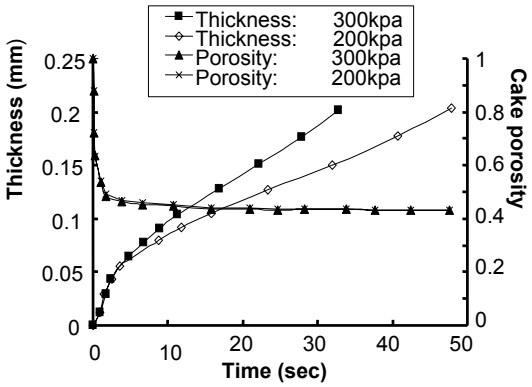

Figure 8. The effect of pressure drop on cake thickness and porosity when $D_p = 20$ μm, $\rho_f = 1.0 \times 10^3$ kg/m^3, $\mu_f = 0.001238$ kg/ms, $H_a = 5.7 \times 10^{-21}$ J, $U_{f,0} = 0.01$ m/s.

Cake structure

The structure of the formed cake and the effect of particle and liquid properties on the structure are discussed in this section. As the first step, only cakes formed by sedimentations are examined in this paper. Porosity, a common parameter for describing a packed bed, is used to identify the cake structure.

Figure 9 shows the effect of Hamaker constant on cake porosity. It shows that: (i) porosity increases with the decreasing particle size when particle size is less than a certain value, which is similar to the packing of particles in air (Yang et al., 2000); (ii) a large Hamaker constant results in a large porosity, which further confirms that a high van der Waals force will result in a loose cake structure; and (iii) the van der Waals force plays a more important role in the liquid than in air. This can be seen when comparing the packings formed in the liquid (sedimentation) and in air. Although in both cases the Hamaker constant is 6.5×10^{-20} J, porosity has increased much more for cakes as particle size decreases.

Figure 10 shows the increase of cake porosity with the increase of liquid density when the van der Waals force exists ($H_a \neq 0$). However, if the van der Waals force is

ignored, cake porosity will have little change. Therefore the van der Waals force is the ultimate reason for the rise of the cake porosity while the increase of liquid density will magnify the effect of van der Waals force, especially when the liquid density is close to the particle density because the buoyancy force counteracts most of the gravity force. As the gravity force decreases rapidly with particle size, smaller sized particles will receive a higher increase in porosity as liquid density increases, as seen in this figure.

Liquid viscosity is another important parameter affecting the cake structures. From Fig. 11 it can be seen that the increase of viscosity will yield an increase in cake porosity. Importantly, the existence of the van der Waals force is a prerequisite. This is obvious when examining the results simulated when Hamaker constant is zero. As shown in Fig. 11, cake porosity is not sensitive to viscosity in this case. Unlike the buoyancy force, the drag force improves the effect of van der Waals force by restricting the movement of the particles and hindering the rearrangement of particles during the accretion of cakes. This will cause the cakes to form a loose structure. Also from the figure we can see that with different liquid densities, the effect of liquid viscosity is different.

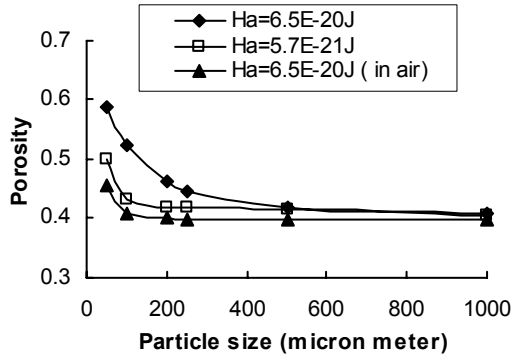

Figure 9. Porosity as a function of particle size for different Hamaker constant when $\rho_f = 1.0 \times 10^3 kg/m^3$, $\mu_f = 0.001238$ kg/ms.

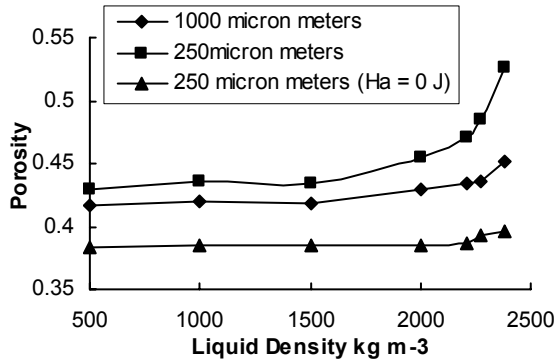

Figure 10. Cake porosity as a function of ρ_f when μ_f=0.001238 kg/ms, $H_a = 5.7 \times 10^{-21}$ J.

To further examine the effects of liquid properties, the evolution of the three liquid related forces during a settling process has been traced, as shown in Fig.12, where the forces at a given time are obtained by averaging those on all the particles). As expected, the buoyancy force remains unchanged. The lift force in the settling process is almost negligible. While the drag force increases rapidly to the limit of the effective gravity force (defined as the gravity force subtracted by the buoyancy force), and then decreases to zero, with some small fluctuations. The increase of liquid viscosity will give rise to the drag force and cause the cakes to be looser. However, unlike the buoyancy force, the drag force will decrease to zero when a stable cake is formed and will not exist in the final states of cakes.

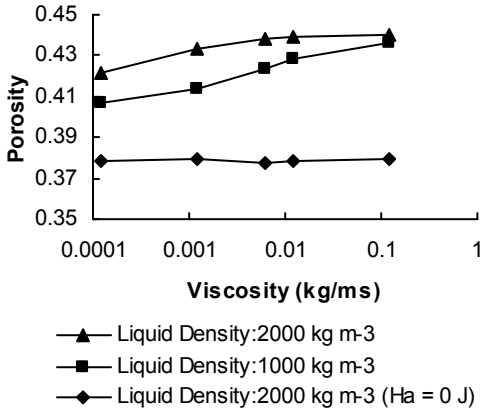

Figure 11. Porosity as a function of liquid viscosity for different liquid density when $D_p = 1$ mm, $H_a = 5.7 \times 10^{-21}$J.

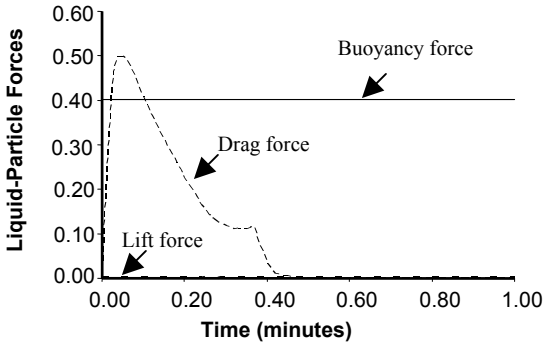

Figure 12. The evolution of liquid-particle force during the sedimentation process when $D_p = 1$ mm, $\rho_f = 1.0 \times 10^3$ kg/m^3, $\mu_f = 0.001238$ kg/ms, $H_a = 5.7 \times 10^{-21}$J

For particles packing in air, it has been found that its porosity can be related to the force ratio of van der Waals force to the gravity force (Yang, et al. 2000). Because of the involvement of the buoyancy force, we use the concept of effective gravity force. Thus, two force ratios are used in this work for quantitative analysis, defined by:

$$\chi = |\sum_j \mathbf{F}_{ij}^v| / |\mathbf{F}_{g,effective}| \quad (17)$$

and

$$\chi' = \sum_j \left|\mathbf{F}_{ij}^{v}\right| / |\mathbf{F}_{g,effective}| \quad (18)$$

Figure 13 shows porosity, ε, as a function of the force ratios, where the lines are generated from the equations formulated in our previous work of particle packing in air (Yang et al. 2000). It clearly shows that our present data agree quite well with the previous analysis. Therefore the result further supports the argument that there is a general relationship between porosity and interparticle force for commonly used particles, as proposed by Yu et al. (2003).

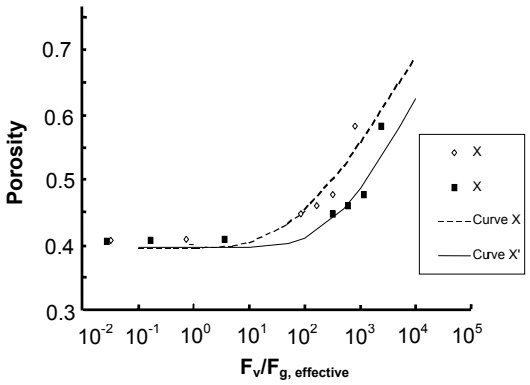

Figure 13. Porosity of final states as a function of force ratio.

CONCLUSIONS

- The DEM simulation model has been successfully extended to the process of sedimentation and filtration. Cake formation and growth in these processes have been studied by numerical experiments.
- Effects of particle size, liquid density, liquid viscosity and Hamaker constant on the cakes have been examined numerically. It is found that the increase of Hamaker constant, liquid viscosity, liquid density and the decrease of particle size will increase the cake porosity.
- The van der Waals force is identified as the most important force controlling the cake structure while other liquid-particle forces such as buoyancy and drag forces can enhance this effect. In general, cake porosity increases with the increase of the van der Waals force relative to the effective gravity force.

ACKNOWLEDGEMENT

The authors are grateful to Australian Research Council and Alcoa for financial support.

REFERENCES

BRILLIANTOV, N. V. and POSCHEL, T. 1998. "Rolling fricition of a viscous sphere on a hard plane." *Europhysics Letters* 42 (5): 511-516.

BRILLIANTOV, N. V., SPAHN, F., HERTZSCH, J. M. and POSCHEL T. 1996. "Model for collisions in granular gases." *Physics Review E* 53 5382

BURGER, R., CONCHA F., KARLSEN K. H., 2001. "Phenomenological model of filtration processes: 1. Cake formation and expression." *Chemical Engineering Science* 56 4537-4553.

CROWE, C., SOMMERFELD, M., and TSUJI, Y. 1998. *Multiphase Flows with Droplets and Particles*. New York: CRC Press

GARRIDO, P., BURGER, R., CONCHA F.. 2000. "Settling velocities of particulate systems: 11. Comparision of the phenomenological sedimentation-consolidation model with published experimental results." *International Journal of Mineral Processing* 60 213-227.

HOUI, D. and LENORMAND, R., 1986. *Experimental and Theoretical Study of Particle Accumulation at the Surface of a Filter*. 4th World Filtration Congress, Ostend, Belgium:

Hwang, K. J. and Lu, W. M. 1995. "Cake Formation in 2-D Cross-Flow Filtration." *AIChE Journal* 41 1443-1455.

ISRAELACHVILI, J. N. 1991. *Intermolecular and Surface Forces*. London: Academic

JOHNSON, K. L. 1985. *Contact Mechanics*. Cambridge: Cambridge University Press

LANGSTON, P. A., TUZUN, U. and HEYES, D. M. 1995. "Discrete element simulation of granular flow in 2D and 3D hoppers: dependence of discharge rate and wall stress on particle interactions." *Chemical Engineering Science* 50 (6): 967

LU, W. M., HWANG, K. J. and JU, S. C.. 1993. "Studies on the Mechanism of Cross-Flow Filtration." *Chemical Engineering Science* 48 863-872.

LU, W. M., HWANG, K.J., 1993. "Mechanism of Cake Formation in Constant Pressure Filtration." *Separation Technology* 3 122-132.

ONODA, G. Y. and LINIGER, E. G. 1990. "Random Loose Packings of Uniform Spheres and the Dilatancy Onset." *Phyiscal Review Letters* 64 (22): 2727-2730.

SVAROVSKY, LADISLAV. 2000. *Solid-Liquid Separation*. London: Butterworth Heinemann

TASSOPOULOS, M., O'BRIEN J. A. , ROSNER D. E.. 1989. "Simulation of Microstructure/Mechanism Relationships in Particle Deposition." *AIChE Journal* 35 967-980.

TIEN, C. 2002. "Cake filtration research - a personal view." *Powder Technology* 127 1-8.

XU, B. H., YU, A. B, CHEW, S. J. and ZULLI, P. 2000. "Numerical simulation of the gas–solid flow in a bed with lateral gas blasting." *Powder Technology* 109 (1-3): 13-26.

YANG, R. Y., ZOU, R. P. and YU, A. B. 2000. "Computer simulation of the packing of fine particles." *Physical Review E* 62 (3): 3900-3908.

YU, A. B., FENG,C. L. , ZOU , R. P. and YANG, R. Y. 2003. "On the relationship between porosity and interparticle forces." *Powder Technology* 130 70-76.

YU, A. B., XU, B. H. 2003. "Particle-scale modeling of gas-solid flow in fluidization." *J. Chem. Technol. Bio.* 78 111-121.

ZHAO, Y., Davis, R. H.. 2002. "Interactions of two touching spheres in a viscous fluid." *Chemical Engineering Science* 57 1997-2006.